Grid-based Exploration of OCT Thickness Data of Intraretinal Layers

Martin Röhlig[1], Jörg Stüwe[1], Christoph Schmidt[1], Ruby Kala Prakasam[2], Oliver Stachs[2] and Heidrun Schumann[1]

[1]*Institute of Computer Science, University of Rostock, Albert-Einstein-Str. 22, Rostock, Germany*

[2]*Department of Ophthalmology, University of Rostock, Doberaner Str. 140, Rostock, Germany*

Keywords: Visual Analysis of OCT Data, Optical Coherence Tomography, Modified ETDRS Grids, Intraretinal Layers.

Abstract: Optical coherence tomography (OCT) enables high-resolution 3D imaging of the human retina to understand a variety of retinal and systemic disorders. Commonly, the thickness of segmented intraretinal layers is used to assess the condition of the retina. However, the thickness data are complex and thus, need to be considerably reduced prior to further processing and analysis. This leads to a loss of information and may hinder the discovery of subtle and localized retinal changes, which are important for an early detection of certain diseases. On this account, we propose an enhanced grid-based reduction of OCT thickness data. We adapt established grid types for retinal thickness data and suggest alternative grids that capture more information. We integrate our data reduction approach into a visual analysis tool that supports an automated computation and interactive exploration of different grids. We demonstrate the application of our tool and show how it can be used to support experts in choosing and comparing appropriate grid representations for given OCT thickness data.

1 INTRODUCTION

Optical coherence tomography (OCT) is a widely-used noninvasive technique to capture high-resolution 3D images of retinal substructures. Ophthalmologists analyze the resulting data to understand a variety of retinal and systemic disorders, e.g., diabetic retinopathy, age-related macular degeneration, and glaucoma. Particularly, the thickness of segmented intraretinal layers is used to assess the condition of the retina. However, derived thickness data are complex, as one thickness value is typically computed for every single point of each intraretinal layer. On the one hand, this enables a spatially precise judgment of the layers. On the other hand, the large amounts of thickness values are difficult to deal with, and a general summary of thickness changes in larger retinal areas is missing. Hence, ophthalmologists typically rely on considerable data reduction prior to further processing and analysis of the data.

Established data reduction approaches for OCT thickness data are commonly based on retinal grids. These grids are used to spatially divide the retina into few large regions and to derive aggregated thickness measures for each region. This helps to get a quick overview of the layers' thickness in anatomically predefined areas. Moreover, it drastically reduces the amount of information to be analyzed, particularly if the layer thickness in larger studies with dozens or hundreds of OCT datasets has to be evaluated. Yet, due to the spatial aggregation, information loss may occur. This is because small and localized variations in thickness are not always reasonably represented via aggregated values of large regions. Capturing such information is, however, mandatory for detecting early signs of certain diseases or investigating progressions.

We aim at supporting ophthalmologists in their grid-based visual analysis of intraretinal layer thickness. We propose an enhanced data reduction scheme together with a visual analysis tool for the exploration of alternative grids. Our approach helps to strike a balance between obtaining a compact grid representation of thickness data and being able to capture more relevant information of intraretinal layers. Our contributions are:

New Grid Design: We propose an enhanced grid-based reduction scheme for OCT thickness data. New grid layouts are derived based on radial and sector-wise subdivision of well-established grids.

Data-driven Adaptation: We introduce a procedure to compute the suitability of different grid layouts for given thickness data. The grids are rated and best options are suggested to the user.

Röhlig, M., Stüwe, J., Schmidt, C., Prakasam, R., Stachs, O. and Schumann, H.
Grid-based Exploration of OCT Thickness Data of Intraretinal Layers.
DOI: 10.5220/0007580001290140
In *Proceedings of the 14th International Joint Conference on Computer Vision, Imaging and Computer Graphics Theory and Applications (VISIGRAPP 2019)*, pages 129-140
ISBN: 978-989-758-354-4

Grid-based Exploration: We develop a new visual analysis tool for grid-based exploration of thickness data. Grids are interactively adjusted, compared to other grids of different datasets, and grid-related details are investigated on demand.

2 BACKGROUND

Our work is motivated and driven by advances in the detection of retinal diseases. Particularly, the dynamic development of OCT technology with respect to image quality, e.g., the improvement of the axial and lateral resolution, offers a unique possibility of differentiating and precisely measuring substructures of the retina. Modern OCT devices are able to capture even subtle retinal changes and allow to accurately monitor the progression of a disease. Based on the data, ophthalmologists aim at performing both:

- *Patient-specific* assessments of the retinal condition of individuals
- *Group-specific* evaluations of experimental and prospective studies in ophthalmic research

In this context, they often need to compare multiple intraindividual datasets, e.g., follow-up examinations of a single patient, and interindividual datasets, e.g., examinations of patients in relation to normative data of controls. Yet, the data analysis can be complex and the available analysis methods differ between existing software tools. In this regard, our work is related to the visual analysis of retinal OCT data in general, and to the representation of retinal layer thickness via grids in particular.

2.1 Visual Analysis of OCT Data

Current analysis procedures are based on a combination of commercial OCT software, non-commercial OCT software, and general-purpose analysis software. Segmentation of intraretinal layers and measurement of layer thickness are supported by both commercial software and non-commercial software (Garvin et al., 2009; Mayer et al., 2010; Mazzaferri et al., 2017). Commercial OCT software is commonly distributed by OCT device manufactures. Currently, several major platforms are available, including software from Nidek, Optovue, Zeiss, Topcon, Heidelberg Engineering and others. The provided software platforms are predominantly used in clinical practice as well as for ophthalmic research. Besides commercial software, few approaches for visually analyzing retinal OCT data exist. Examples are the research-oriented Iowa Reference Algorithms (Garvin et al., 2009), the open-source software ImageJ (Schindelin et al., 2015) and its application to OCT data (Garrido et al., 2014), a 3D visualization of OCT data based on ray-tracing (Glittenberg et al., 2009), and a recent visual analysis framework based on multiple coordinated views (Röhlig et al., 2018). These software tools are typically applied in ophthalmic research. In general, all available analysis software packages support at least one of three fundamental presentation methods for OCT data: cross-sectional views, 3D views, and top-down views.

Cross-sectional views show individual 2D image slices of volumetric OCT data together with overlaid profiles of segmented intraretinal layers. This allows to view details but flipping through the images is time-consuming, as OCT datasets can consist of hundreds of slice images. *3D views* show an entire OCT dataset as a 3D volume rendered tomogram. This provides an overview of the data but combined 3D visualizations of the tomogram and the layers are only provided by few tools, e.g., (Röhlig et al., 2018). *Top-down views* show a fundus image of the interior surface of the eye around the OCT acquisition area together with superimposed retinal layers. This facilitates a layer-centric analysis of the data and helps to link the layers to retinal areas in the fundus image. In general, cross-sectional views and 3D views are mainly used for the visual analysis of individual datasets, whereas top-down views are also applied to anatomically localize and compare areas under investigation in multiple OCT datasets. In this regard, top-down views are most relevant to our work.

Instead of showing the raw OCT data, top-down views typically represent intraretinal layers via their derived layer thickness. The layer thickness is displayed either via thickness maps or via spatially aggregated thickness grids. This helps to reveal even subtle retinal changes, which may be difficult to identify by visualizing the raw OCT data alone. While there recently have been advances in the application of thickness maps for the analysis of OCT data (Röhlig et al., 2018), thickness grids are still predominantly used in most opthalmic applications. On the other hand, the design of thickness grids has been hardly investigated in previous work, despite the continuous development of OCT technology and associated analysis methods. On this account, we particularly focus on the grid-based exploration of retinal thickness data.

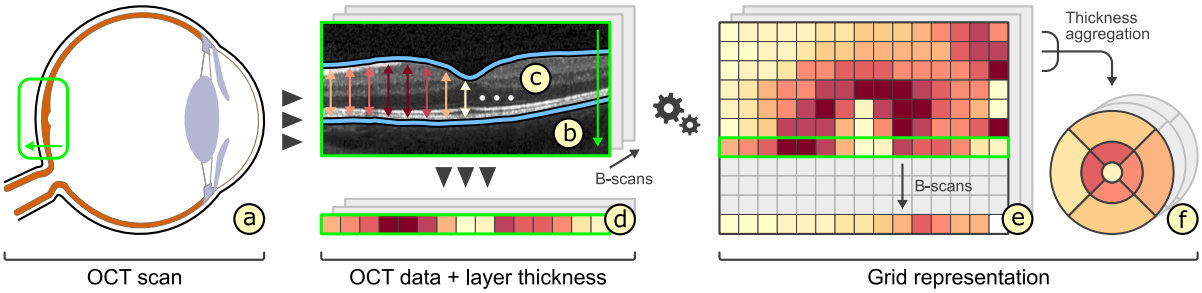

Figure 1: Grid representation of retinal layer thickness. An OCT scan captures the area around the macula and the optic disk (a). The resulting volumetric data consists of multiple 2D image slices (B-scans) (b). Several intraretinal layers are extracted from each B-scan (c) and thickness values are computed for every pixel along the horizontal image axes by measuring the vertical distance between the upper and lower layer boundaries (d). The thickness values are combined across all B-scans per retinal layer (e) and spatially aggregated into corresponding grid representations (f).

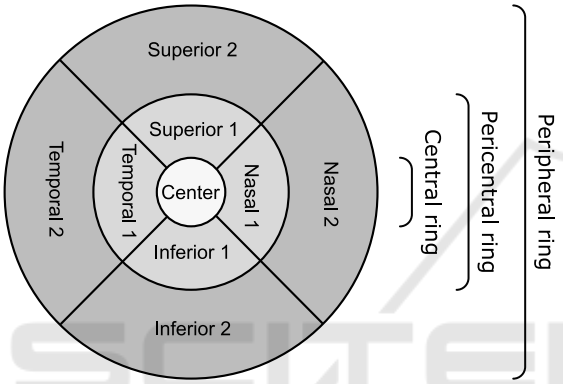

Figure 2: The layout of the ETDRS grid. The grid divides the retina into nine regions defined by three rings, i.e., central, pericentral, and peripheral, and four sectors, i.e., nasal, temporal, superior, and inferior.

2.2 Representation of Retinal Layer Thickness via Grids

The most common grid type to represent retinal thickness data was established by the Early Treatment Diabetic Retinopathy Study (ETDRS) (Chew et al., 1996). The cells of ETDRS grids divide the retina into nine large regions, i.e., a central foveal ring with 1mm diameter, an inner macula ring (pericentral) with 3mm diameter, and an outer macula ring (peripheral) with 6mm diameter. The inner and outer rings are further divided into four quadrants, namely nasal, temporal, superior, and inferior. For each grid cell and intraretinal layer, typically one aggregated thickness measurement is stored. Figure 1 illustrates how such grid representations are obtained and Figure 2 shows the layout of the ETDRS grid. The grid design enables the localization and assessment of anatomically important areas of the macula near the center of the retina. Thus, ETDRS grids have been widely applied for various purposes in ophthalmic research, including investigations of early structural changes of the retina for a variety of diseases, e.g., diabetes mellitus (Götze et al., 2018) and glaucoma (Chen et al., 2017). Although other grid types exist, they have been mostly designed for special applications, e.g., rectangular grids for asymmetry analysis of retinal thickness for glaucoma diagnosis (Asrani et al., 2011).

A major advantage of ETDRS grids is their compact representation of the complex thickness data with only few aggregated values for each intraretinal layer, i.e., typically one arithmetic mean thickness value per grid cell. This allows a quick overview and judgment of thickness changes in predefined retinal areas. Moreover, the applied data reduction eases the evaluation and comparison of multiple datasets. Particularly in case of larger studies, it is easier to handle fewer data values for statistical analysis and interpretation of the data. That is because ophthalmologists conventionally export ETDRS thickness values from OCT software to external spreadsheet software or statistics software to compile study groups and to perform batched or non-batched statistical analyses. On top of that, the fixed grid cells enable the comparison of results from different studies that used ETDRS grids.

On the downside, the main problem with ETDRS grids is that they do not necessarily faithfully represent underlying thickness data (Fig. 3). Due to the considerable spatial data reduction, localized variations in thickness of an intraretinal layer are not accurately captured via a single aggregated thickness value per grid cell. This is the case for both small variations in thickness within a grid cell and variations divided by the boundary of two or more grid cells (Fig. 3c). Moreover, when evaluating deviations between thickness data of multiple OCT datasets, aggregation artifacts may bear an additional risk of information loss. The reason for this is that localized positive and negative deviations within a grid cell may be nullified during data reduction (Fig. 3g). This can

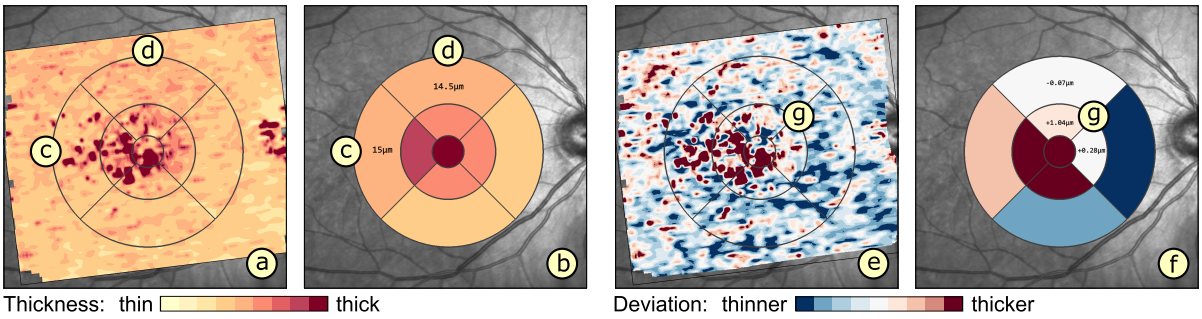

Figure 3: Data representation with ETDRS grids. The thickness of an intraretinal layer is shown via a thickness map (a) and an ETDRS grid (b). Small and localized regions of high thickness (dark red) in the map are not accurately represented in all cells of the grid, e.g., cell (c) with regions of high thickness has almost the same aggregated value as cell (d) without such regions. In addition, localized regions of positive and negative deviations in thickness (dark red and dark blue) in the map (e) are nullified in certain cells of the grid (f), e.g., averaging artifacts of grids cells (g).

lead to false normal findings. Detecting such information is, however, vital for the identification of early retinal changes of certain diseases.

3 GRID DESIGN

Given both the discussed benefits and drawbacks of ETDRS grids, we aim at designing alternative grids that combine the advantages of ETDRS grids with the possibility to capture more relevant information. To this end, we identified design requirements, devised a new subdivision scheme that allows to compare different grid layouts, and developed a method to rate the representation quality of grids for given data.

3.1 Requirements

The grid-related design requirements reflect the experts' needs with regard to processing and analyzing OCT thickness data. We derived the following list by talking with the experts about current limitations and about the way they utilize existing grids to analyze thickness data of intraretinal layers.

Layout based on ETDRS Grid (GR_1): The basic layout of alternative grids should correspond to the ETDRS grid. This is to maintain the ability to localize anatomically important areas of the macula near the center of the retina.

Compact Data Representation (GR_2): In general, the number of grid cells should be small and the content of a grid cell should be mainly represented by only a single descriptive value. Nevertheless, an appropriate representation of thickness data should be facilitated.

Compariability of Grid Layouts (GR_3): Alternative grid layouts should be comparable to both the basic ETDRS grid and other alternative grids. This is to ensure that analysis results from multiple datasets with different grids are relatable.

3.2 Subdivision of Grids

Based on the experts' demands, we design alternative grids that meet requirements GR_1 and GR_2. Our approach is based on subdivisions of existing grid layouts. Taking the ETDRS grid as a basis, we employ a radial or a sector-wise partition strategy of ETDRS grid cells. This allows us to obtain alternative grids that represent the underlying thickness data at different levels of granularity. Figure 4a exemplifies both partition strategies.

Radial partitions add rings to a grid. The resulting grid cells enable a more fine-grained analysis of areas with respect to the distance from the foveal center. For example, intraretinal layer thickness of macula rings can be investigated in-depth via secondary pericentral or peripheral cells. *Sector-wise partitions* add separating lines at certain angles to a grid. The generated grid cells facilitate a more direction-centric analysis of areas with respect to the foveal center. For example, by adding further directional cells, the thickness of areas facing nasally may be evaluated in greater detail in relation to areas facing temporally. Radial and sector-wise partitions can also be combined to obtain fine grids that support analyses with focus on both properties.

To restrict the number of all possible combinations of subdivisions, we suggest to start by equally dividing grid cells and to increase the number of radii or sectors in power of two steps. By dividing grid cells in half for each radial or sector-wise subdivision

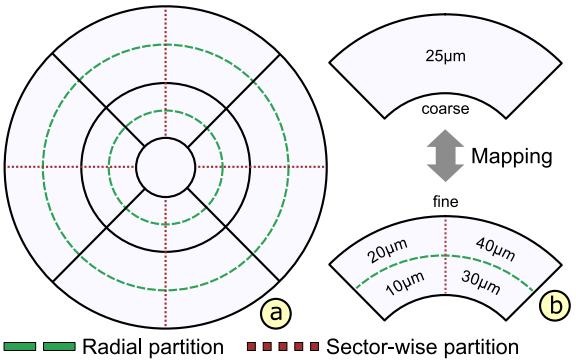

Figure 4: Subdivision and mapping of grids. The ETDRS grid layout is subdivided via radial (dashed line) or sector-wise (dotted line) partitions to derive alternative grids (a). To ensure the comparability of grids, a coarse grid is mapped to a fine grid or vice versa by subdividing or merging corresponding grid cells (b).

pass, the amount of information stored in a subdivided grid is increased in constant steps. The resulting set of grids can then be refined interactively. Just like conventional ETDRS grids, we represent the content of each grid cell via one aggregated thickness measurement. Optionally, additional summary statistics, e.g., mean, percentiles, and standard deviation, may be stored per cell to provide further information on the distribution of the underlying thickness data.

Utilizing the well-known ETDRS grid as a basis for radial or sector-wise subdivisions helps experts to familiarize themselves with the layout of derived grids. The simple and fixed subdivision scheme eases the localization of areas under investigation and the interpretation of the data. This in turn increases the acceptance of alternative grids. Next, we discuss how to further support experts in choosing an appropriate grid from a set of alternatives for their given data.

3.3 Rating of Grids

In general, no single grid layout exists that fits all possible spatial distributions of thickness data. Instead of trying to create such an all-solving solution, we provide a set of alternative grids to choose from. Yet, given all available grid layouts, experts now face the problem that they have to decide which grid actually matches their given data. To support experts in this decision, we developed a rating procedure based on a quantitative measure of the representation quality for each grid under consideration. With our rating of grids we are able to address the second aspect of design requirement GR_2.

We determine the overall representation quality of a grid by measuring the homogeneity of thickness values of all data points within each grid cell. This is based on the assumption that a cell with high homogeneity covers thickness values that are more or less equal, whereas a cell with low homogeneity encloses strongly varying thickness values. Thus, an aggregated thickness value of a grid cell with high homogeneity matches the thickness values within that cell. In contrast, a cell with low homogeneity indicates information loss, e.g., due to averaging of localized variations. Consequently, a grid composed of cells with high homogeneity corresponds to a good representation of the underlying thickness data and vice versa.

One possible measure to quantify the amount of variation or homogeneity of a set of thickness values inside a grid cell is the standard deviation. Based on this simple measure, we obtain the overall rating of a grid via the weighted arithmetic mean of the computed standard deviations of all grid cells.

$$\bar{x} = \frac{\sum_{i=1}^{n} w_i x_i}{\sum_{i=1}^{n} w_i}$$

In this equation, $\bar{x}$ represents the final rating of the grid, n denotes the number of grid cells, x_i is the standard deviation of a cell, and w_i is the weight for that cell given by the normalized amount of enclosed data points (equal to the size of the cell). Based on the final ratings, we compute a ranking for a set of alternative grids and suggest a best fit for thickness data of one retinal layer while considering secondary expert constraints. Such constraints are a specified maximum number of allowed grid cells or a preference for either radial or sector-wise subdivisions. This promotes a more patient-specific analysis in contrast to generalizing all given thickness data to just the ETDRS grid representation. Likewise, the rating and ranking can be adapted to support a group-specific assessment of grids. The procedures allow to find one best fitting grid for multiple layers of one dataset or even for one or several layers of multiple datasets, e.g, to obtain one grid to represent the data of all patients in a study. The resulting rankings are then used to steer the grid-based visual exploration of thickness data.

3.4 Comparability of Grids

Ophthalmologists are often interested in relating grid-based analysis results from multiple datasets (cf. GR_3). In a patient-specific analysis scenario, each of these individual datasets may be best represented by another grid with a different layout. To ensure the comparability of the grids, we support mapping a fine grid to a coarse grid and vice versa. This is possible as in our design a fine grid is basically a subdivided version of a coarse grid. Figure 4b illustrates both mapping strategies. In addition, in a group-specific

analysis scenario, grids of a patient group may have to be compared to grids of another patient group or of a control group. On this account, we allow to compile a set of multiple source grids of a group into a single aggregated grid. The aggregated grid cells can then be mapped and assigned values can be directly related.

Mapping a fine grid to a coarse grid entails that subdivided grid cells have to be merged together to the granularity level of the cells of the coarse grid. The values of the merged cells are determined by aggregating the values of the corresponding subdivided cells, e.g., by computing and storing their arithmetic mean. The most prominent example for this mapping strategy is to trace alternative grids back to the initial ETDRS grid. As a practical example, this allows to compare new analysis results obtained via our grid design to results of previous ophthalmic studies based on the ETDRS grid. Another example is to select the coarsest subdivision grid from a set of alternatives as reference and to map the other grids to that reference. This is necessary if the underlying thickness data are no longer available and thus, merging finer cells and aggregating associated values are the only options.

Mapping a coarse grid to a fine grid involves that coarse grid cells are subdivided to the granularity level of the cells of the fine grid. The values of the subdivided cells are then assigned either by recomputing them based on the underlying thickness data or simply by copying the values of corresponding coarser cells. A precondition for the second case is however that the coarse grid is a good representation of that data and consequently, a subdivided version of that grid represents the data equally well, i.e, it just consists of more grid cells. An advantage of this mapping strategy is that no details stored via finer grid cells are lost during the comparison. Practically this is important if, for example, a fine grid representing a patient with abnormal localized variations in thickness has to be compared to a coarser grid representing normative data of healthy controls, which commonly show less variations in thickness and only in larger areas.

Compiling an aggregated grid implies that multiple source grids are transformed into a single grid representation. First, a layout for the aggregated grid is determined and then the source grids are mapped to that common layout. The aggregated grid represents the source grids via one descriptive value per cell, e.g., the arithmetic mean of corresponding source cell values. In addition, summary statistics of source values may be stored per aggregated grid cell. To analyze two or more aggregated grids, they are mapped using one of the above strategies and related based on corresponding cell values. This way, a grid of a single patient or an aggregated grid of a patient group can be compared to an aggregated grid of a control group.

In summary, our grid design allows to obtain compact representations of retinal thickness data comparable to well-established ETDRS grids, while also being able to capture more relevant information. Thus, our solution is a first step towards supporting ophthalmologists in choosing thickness grids that fit the OCT data under investigation. In addition, we designed an interactive visualization tool that supports the exploration of different grids and adjusting their visual representation.

4 GRID-BASED VISUAL EXPLORATION

We aim at supporting users in their grid-based analysis of OCT thickness data of intraretinal layers. For this purpose, we design a visualization tool based on multiple coordinated views. Figure 5 shows an overview of the user interface. Our tool supports: (i) visualizing grids, (ii) showing grid details on demand, (iii) interactively adapting grids to facilitate exploration, and (iv) comparing different grids.

4.1 Presentation of Grids

In order to enable a comprehensive analysis of thickness grids, we visualize different grids together with related information. To this end, we design a top-down view for coloring and labeling of grids and a measurement view for showing details of grid cells.

The *top-down view* provides an overview of different thickness grids with regard to the interior surface of the eye (Fig. 5a). A fundus image depicts the OCT acquisition area. Colored grids of selected intraretinal layers are visualized on top of the fundus image. The opacity of the grid overlay can be adjusted using a slider to help to relate attribute values in the maps to noticeable structures in the subjacent fundus image. All other intraretinal layers are shown as grid thumbnails on the side, ordered according to their anatomical location within the retina (Fig. 5c). This view design presents grids for all layers in one image without having to flip through them manually. Thus, layers with abnormal characteristics can be easily discovered.

The *coloring of grids* is based on suitable and adjustable palettes (Harrower and Brewer, 2003). Sequential palettes encode the actual thickness of individual grids or the averaged thickness of aggregated multiple grids. The cells are colored by evaluating the stored thickness values with respect to clinically established thresholds. Two boundary values are given for all cells of each retinal layer. Low thickness

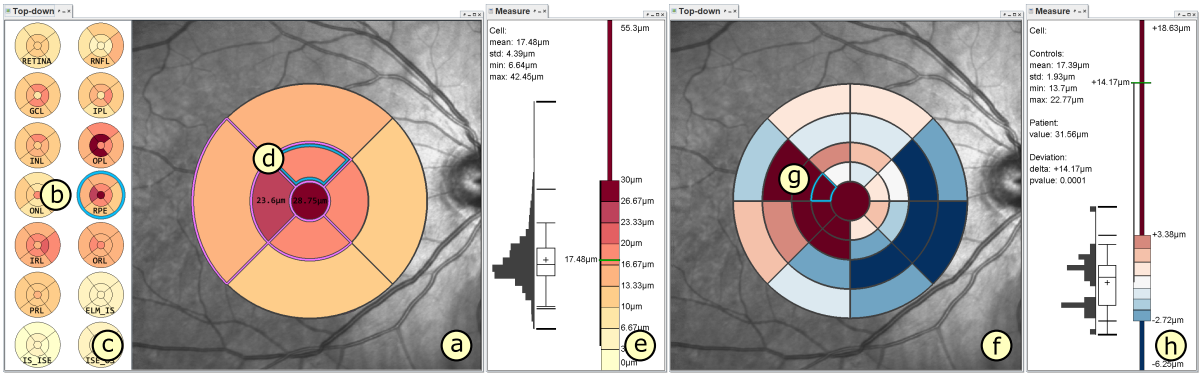

Figure 5: Overview of our prototypical visual analysis tool. In the left top-down view (a), an intraretinal layer (b) is selected in the layer overview (c) and the associated thickness grid is enlarged and superimposed over a fundus image. Aggregated thickness values per cell are color-coded, labels indicate cell values close to specified thresholds, and borders of cells with low ratings are highlighted (purple). Details about the underlying thickness data of a selected grid cell (d) are shown in a linked measurement view (e). In the right top-down view (f), the selected grid is mapped and compared to reference data of a control group and deviations are color-coded. Details of a selected cell (g) are shown in a second measurement view (h) in relation to the distribution of the reference data.

values are assigned to light colors, high thickness values to dark colors, and thickness values outside the specified thickness ranges to distinctively lighter or darker colors. Figure 5a shows an example. This allows to judge the thickness data globally in relation to the given boundaries. The coloring on the basis of common thresholds also allows to relate grid presentations across different datasets.

The *labeling of grids* enriches the colored grid presentation with additional text labels and highlighted cell borders. Text labels are added to show values of grid cells in detail. Optionally, only text labels of selected cells or of cells with values outside of specified thresholds are displayed. This is to prevent visual clutter in the image, particularly in fine grids with a lot of small cells. Instead of showing numeric cell values, the textual labeling can be switched to encode location-oriented cell names. To this end, existing naming conventions of the ETDRS grid (cf. Fig. 2) can be adapted to derived grids, e.g., by adding suffixes like pericentral inner or outer for radially partitioned cells. Alternatively, naming schemes based on notations of time and partial distances can be applied. For instance, the location of a cell is denoted by *11:0.25*, which stands for a cell in the direction of the 11th hour on a 12-hour clock at one-quarter of the distance between the foveal center and the outer macular border. Next to text labels of cells, cell borders are outlined to illustrate the structure of grids and to highlight specific cells. By default, all cell borders are outlined. This presentation can be adjusted to match selectively shown text labels of abnormal cells or to mark the ETDRS grid layout in subdivided grids (Fig. 6a). This further facilitates the localization of cells. Finally, cell borders may be emphasized to reflect the computed rating of grid cells, e.g., to indicate information loss in cells with low homogeneity (Fig. 6b).

The *measurement view* helps to go beyond the basic grid presentation and to show further details about the underlying thickness data (Fig. 5e). Thickness values of selected cells in the top-down view are visualized as lines and numerical text labels on top of a color legend in the measurement view. The legend reflects the applied coloring and specified thresholds of the grid presentation. Next to the legend, summary statistics associated with selected cells are optionally shown as statistical plots. For individual grids, the distribution of the contained thickness data is visualized via box-and-whisker plots and histograms together with numerical labels of descriptive values. This helps to judge the grid representation and to understand the rating of cells, e.g., by showing the distribution of highlighted cells with low homogeneity. For aggregated grids, the statistical plots encode the distribution of thickness values assigned to corresponding cells of all source grids. This allows to assess the variability of thickness values of a group of patients.

4.2 Interactive Exploration of Grids

To promote an in-depth analysis of retinal thickness data, the data have to be explored at appropriate level of granularity. We support users in specifying initial grids to start the exploration, browsing through grids at different levels of granularity, adapting grids on demand, and comparing different grids.

Specifying initial grids is possible via interactive grid design and based on automated grid suggestions. To interactively design a grid, the respective layout parameters, i.e., the number of radii and sectors, have

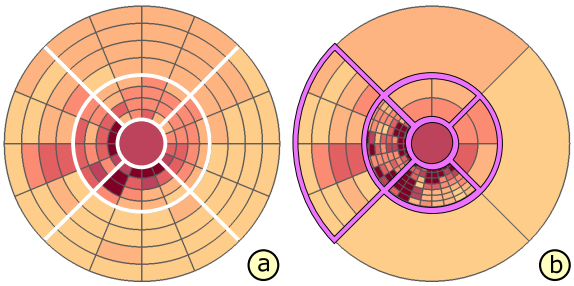

Figure 6: Interactive exploration of grids. The ETDRS grid layout is marked on a subdivided grid to support the localization of cells (a). Grid cells with low ratings (purple borders) are interactively subdivided to investigate details (b).

to be set. This first option offers the most freedom to the expert and allows to obtain a set of grids that reflects specific needs. The second option is to automatically suggest fitting grids for given thickness data based on the computed rating and ranking of a predefined set of alternative grid layouts. Such a predefined set of alternatives may consist of increasingly finer subdivisions of the ETDRS grid using combinations of both radial and sector-wise partition strategies. An expert may further steer the automated selection by setting additional constraints, e.g, the maximum number of allowed grid cells. This helps to obtain grids at an appropriate level of granularity, i.e., grids that capture even small and localized variations in thickness.

Browsing through grids is supported by interactive selections from a set of specified grid layouts. Selected grids are immediately presented in the top-down view with cells colored and labeled. By flipping through these grids, the data can be explored at different levels of granularity. For instance, selecting increasingly finer subdivision of the ETDRS grid allows to analyze the data from overview, i.e., coarsest grid, to detail, i.e., finest grid. This helps to understand the data and to localize areas of interest.

Interactively adapting grids allows to refine a selected grid layout. On demand, one or multiple grid cells may be selected and then merged together or subdivided by means of the provided partitioning strategies (cf. Sect. 3.2). This helps to fine-tune grids for given data based on the expertise of experts. For instance, while browsing through alternative grids, a specific grid is selected, cells are visualized, and information about the underlying thickness data is shown. Individual grid cells with low ratings are then further subdivided to investigate respective areas in greater detail and the remaining cells are merged together to provide context information of less relevant areas. Figure 6b exemplifies the adaption of grids.

Comparison of different grids is enabled by juxtaposition of views, explicit encoding of deviations, and application of statistical tests. The juxtaposition of

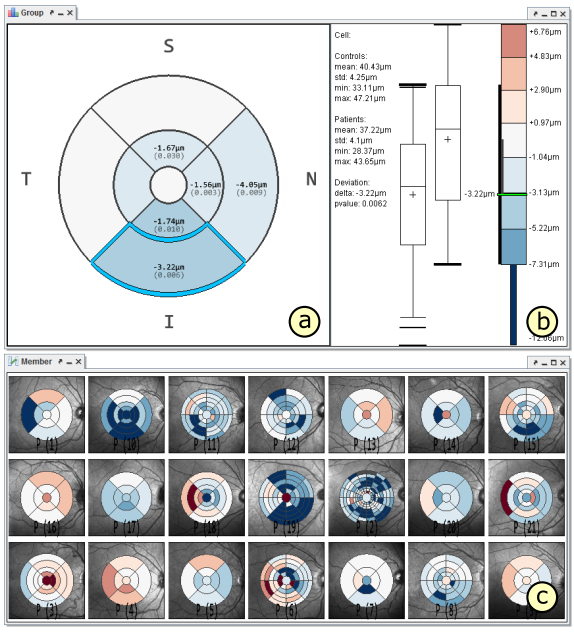

Figure 7: Comparison of different grids. The top-down view (a) and the linked measurement view (b) show a group-specific comparison of an aggregated grid of a patient group to an aggregated grid of a control group. The juxtaposed small multiple views (c) show an overview of grids of all individual members of the patient group compared to the aggregated grid of the control group. Thickness deviations are explicitly encoded using a diverging color palette.

views supports the comparison of several individual grids (Fig. 5a, f). In the user interface, multiple instances of the top-down view and measurement view can be dynamically added and freely arranged. For a patient-specific analysis, different grids of the same patient, e.g., follow-up examinations, or of related patients, e.g., similar medical cases, can be assigned to these view instances. Linking the view instances ensures that matching parts of the data are shown. For a group-specific analysis, individual grids of all members of a group are shown as small multiple views (Fig. 7c). This provides a quick overview and allows to detect differences between group members.

The explicit encoding of deviations facilitates a direct comparison of a grid to a reference grid. For this purpose, the coloring of the grid presentation is switched. The cells are colored using diverging palettes and by evaluating the stored thickness values with respect to threshold intervals of an aggregated reference grid. The boundary values vary cell by cell for each layer, e.g., confidence intervals or percentile boundaries per reference cell. Small deviations from a reference are represented via a light neutral color and larger negative or positive deviations via respective darker colors. Displaying deviations helps to evaluate a thickness grid locally in relation to a reference

grid. Figure 5f and Figure 7a exemplify comparisons of a grid of a single patient and of an aggregated grid of an entire patient group to intervals ranging between the 2.5th and 97.5th percentile boundaries stored in an aggregated grid of a control group, respectively.

The application of statistical tests allows to quantify the differences between multiple aggregated grids. For example, for the comparison of aggregated grids of two different groups, e.g., patients and controls, an independent two-sample Student's *t*-test is applied and for aggregated grids of more groups an one-way analysis of variance is performed. The resulting measurements of statistical significance, i.e., p-values, and effect size are shown as numerical labels. In addition, statistical plots for the cells of each grid under consideration are shown in the measurement view (Fig. 7b). This illustrates the difference between the thickness distributions and provides additional details about the color-coded deviations in the comparative grid presentation. Altogether, the functionality eases the evaluation of studies with a lot of datasets, as this conventionally requires to first export the data of all source grids and then to statistically analyze them using external software (cf. Sect. 2.2).

5 APPLICATION

We applied and evaluated our research prototype in cooperation with domain experts. We particularly aimed at assessing the utility of our solutions in the context of experimental studies. Here, we briefly describe one use case, present exemplary results, and reflect on benefits and limitations of our approach.

5.1 Use Case

In this use case, we applied our solutions to study if early retinal changes in adult patients suffering from age-related macular degeneration (AMD) can be captured via different grid representations. In addition, we were interested in relating the obtained results to grid representations of healthy control subjects.

A common early sign of AMD is the presence of drusen in the macula. Drusen are small accumulations of extracellular material that build up between Bruch's membrane and the retinal pigment epithelium (RPE) of the eye (Yoshimura and Hangai, 2014). The high sensitivity of OCT and the analysis of OCT data support detecting such small and localized changes, and hence may contribute to an early diagnosis and immediate intervention. Yet, in the thickness data of the RPE, these retinal changes are reflected by small

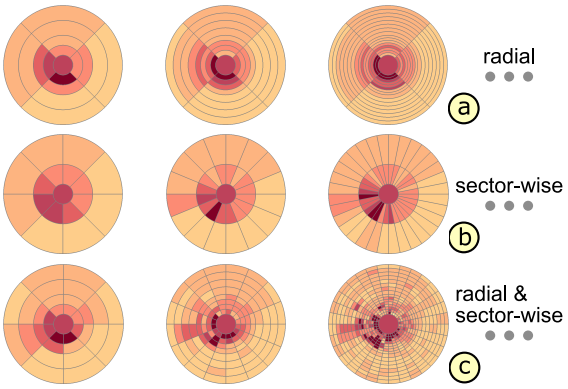

Figure 8: Examples of alternative grids evaluated in our use case. Three partitioning strategies were applied to derive increasingly finer grids: radial (a), sector-wise (b), and radial and sector-wise partitions (c).

and localized increases in thickness. We hypothesize that conventional ETDRS grids may not always accurately represent the thickness data in this situation (cf. Sect. 2.2). In fact, the principal goal of this study was to assess alternative grids for early retinal changes in all datasets of participating AMD patients.

The study data were acquired via OCT examinations of two groups of subjects. The first group consists of 8 adults with AMD and the second group of 20 healthy controls. For each subject, the thickness data of the RPE from one OCT dataset of the macula was selected for further investigation (28 datasets in total). Starting from the ETDRS grid, three partitioning strategies were applied: radial, sector-wise, or radial and sector-wise partitions. The numbers of radii and sectors were increased in constant steps per strategy up to a maximum of 129 radii, 256 sectors, and 17 radii plus 32 sectors respectively. The finest grid had 513 cells for each strategy. In total, a set of 21 grids, i.e., 7 grids per strategy, was defined (Fig. 8). In a preprocess, grid representation were computed and rated for the thickness data of each dataset in both groups. The ratings were then summarized per grid to judge the overall representation quality for each group.

Figure 9 shows an overview of the obtained results. Note that these results are only meant as a proof of concept example to demonstrate the feasibility of our approach. We are aware of the possible bias induced by the small sample size, which prevents drawing any medical conclusions. Nonetheless, from a data-centric perspective, we are able to reason about the utility of our approach and to summarize our insights gained from interpreting the results. In this connection, we assume that a superior data representation is reflected by a better rating of grids using the measures introduced in Sect. 3.3, i.e., a good representation is equal to a low mean standard deviation.

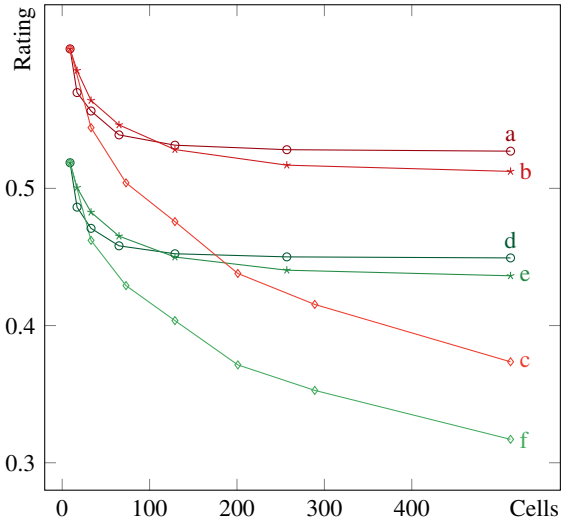

Figure 9: Overview of the study results. The line plot shows ratings of grids, i.e., summarized standard deviations, with respect to cell counts. The ratings are depicted for the thickness data of patients (red) and controls (green) in relation to three partitioning strategies: radial (a, d), sector-wise (b, e), and radial and sector-wise (c, f).

In general, all subdivided grids showed better ratings than the ETDRS grid. For the thickness data of patients, grids based on sector-wise partitions performed slightly better than grids based on radial partitions (Fig. 9a, b). Interestingly, for both partition strategies, an increase in cell count only resulted in better ratings up to a certain point. In contrast, for combined radial and sector-wise partitions, an increase in cell count showed steadily improved ratings (Fig. 9c). A possible explanation is that early drusen often come in the form of small, roughly circular-shaped regions of high thickness. Hence, grid cells that match such shapes, e.g., cells of grids subdivided via combined radial and sector-wise partitions, will result in better overall ratings of respective grids.

For the thickness data of controls, we observed patterns in the grid ratings that are similar to the results of patients (Fig. 9d, e, f). This similarity can probably be explained due to the consideration of patients with early signs of AMD in the study, i.e., while the patients' thickness data showed some noticeable changes, they were still not too far from the data of healthy controls. One remarkable difference was, however, that the control data generally required fewer cells to obtain equally good ratings of grids. This is probably due to the fact that thickness data of healthy eyes contains less localized variations in thickness. Thus, an appropriate grid representation of the data can be achieved with fewer and coarser cells.

5.2 User Feedback and Lessons Learned

Our solutions are the result of a participatory design process starting from prior work (Röhlig et al., 2018). We cooperated with two groups of domain experts, including ophthalmic research scientists and a team of technical and medical professionals from a major commercial OCT device manufacturer. Throughout the development, we had close contact with primarily two ophthalmic experts. Together, we applied and tested our prototype in collaborative data analysis sessions using a pair analytics approach (Arias-Hernandez et al., 2011). We also held repeated demonstration and feedback sessions with around ten participants of both expert groups. We jointly identified challenges and specified respective requirements (cf. Sect. 3.1). Their informal feedback helped us to devise suitable grid designs and visualization techniques.

During the discussions, the experts stated that they liked the visual analysis tool because it allowed them to explore their thickness data at different levels of granularity. They also appreciated the consideration of the established ETDRS grid in our grid design. At the same time, they reassured us that the provided methods for subdivision, rating, and comparability of grids are meaningful enhancements to obtain appropriate data representations. In fact, the experts reported that there is a need to find grids that match certain ophthalmic applications, as existing grids are not always the best choice for their analysis tasks.

In this regard, the results of our experimental study suggest that our approach can be a useful aid for identifying appropriate grids for given thickness data. However, arbitrarily fine subdivided grids are practically unfeasible for some applications. For example, choosing a grid with a large number of cells may impede further utilization of the data. On this account, the experts approved to have the rating and ranking of grids at their disposal. It helped them to decide how much variance they are willing to accept in a grid with a certain amount of cells. They considered such decisions to be particularly easy to make in case of grids that showed only minimally improved ratings in further subdivision with a certain partitioning strategy (cf. Fig. 9). Thus, with the provided functionality, they were able to balance the granularity of grids and the amount of encoded information.

As another major advantage, the ophthalmic experts identified the ability to compare multiple and possibly differing grids with each other and to the conventional ETDRS grid. The interlinked top-down and measurement views helped them to quickly switch between grids of different layers or datasets

and to show grid-related details when necessary. For the analysis of larger studies, they considered the visualization of deviations between aggregated grids of groups and the integrated quantification of differences based on statistical tests to be particular useful. They concluded that reducing the manual analysis effort and being able to obtain results with higher spatial accuracy compared to the current analysis procedures are great benefits.

6 CONCLUSION

We presented an enhanced grid-based data reduction approach for retinal thickness data. A new grid design helps to strike a balance between obtaining a compact data representation and being able to capture more relevant information. A coordinated visual analysis tool supports a grid-based exploration of thickness data at different levels of granularity. Different grids from multiple datasets are compared. Alternative grids are rated and ranked to facilitate the selection of best fitting grids for given thickness data. Our approach constitutes a systematic enhancement of existing work and hence, provides a first step towards supporting ophthalmologists in their grid-based analysis of intraretinal layer thickness.

Our data reduction is based on subdivisions of the widely-used ETDRS grid layout. This allows to address various ophthalmic applications while promoting a more patient-specific analysis. Beyond taking the ETDRS grids as a basis, the main ideas of subdivision, rating, and comparability together with coordinated visualization are applicable to other grid types as well. This may help to support fine-grained analyses in more specific ophthalmic applications, e.g., asymmetry analysis of retinal thickness for glaucoma diagnosis using rectangular grids (Asrani et al., 2011).

During demonstration and feedback sessions, our experts reported that it is not always known which grid helps to solve a given analysis task. Hence, research effort exists to find new grids that adequately represent retinal changes of specific diseases. In this regard, our rating and ranking of grids may help in evaluating newly designed grids and sorting out existing grid types. So far, we used a data-driven approach to judge the representation quality of grids. An interesting extension is to also support diagnosis-driven grid ratings. This requires defining custom measures that match different ophthalmic analysis tasks, e.g. asymmetry analysis of thickness data. Moreover, assistance in choosing suitable rating cutoffs for the selection of grids has to be provided. That way, automated grid suggestions for specific tasks or application are possible. However, to fully support such efforts, more work is needed to be able to compare and rank different grid types.

We ascertained the general utility of our solutions in first tests with domain experts. To improve our design, we plan further evaluations of our tool in the context of experimental studies. In this connection, an interesting open question is how our grid-based analysis approach can be combined with recent map-based analysis approaches for thickness data of intraretinal layers, e.g., (Röhlig et al., 2018). To utilize the benefits of both approaches, identifying and evaluating best practices for each solution is required with respect to an ophthalmic analysis workflow.

ACKNOWLEDGEMENTS

This work has been supported by the German Research Foundation (project VIES).

REFERENCES

Arias-Hernandez, R., Kaastra, L. T., Green, T. M., and Fisher, B. D. (2011). Pair analytics: Capturing reasoning processes in collaborative visual analytics. In *Proceedings of the Hawaii International Conference on System Sciences*, pages 1–10, Washington, DC, USA. IEEE Computer Society.

Asrani, S., Rosdahl, J., and Allingham, R. (2011). Novel software strategy for glaucoma diagnosis: Asymmetry analysis of retinal thickness. *Archives of Ophthalmology*, 129(9):1205–1211.

Chen, Q., Huang, S., Ma, Q., Lin, H., Pan, M., Liu, X., Lu, F., and Shen, M. (2017). Ultra-high resolution profiles of macular intra-retinal layer thicknesses and associations with visual field defects in primary open angle glaucoma. *Scientific Reports*, 7:41100.

Chew, E., Klein, M., Ferris, F., Remaley, N., Murphy, R., Chantry, K., Hoogwerf, B., and Miller, D. (1996). Association of elevated serum lipid levels with retinal hard exudate in diabetic retinopathy: Early treatment diabetic retinopathy study (ETDRS) report 22. *Archives of Ophthalmology*, 114(9):1079–1084.

Garrido, M. G., Beck, S. C., Mühlfriedel, R., Julien, S., Schraermeyer, U., and Seeliger, M. W. (2014). Towards a quantitative OCT image analysis. *PLOS ONE*, 9(6):1–10.

Garvin, M. K., Abramoff, M. D., Wu, X., Russell, S. R., Burns, T. L., and Sonka, M. (2009). Automated 3-D intraretinal layer segmentation of macular spectral-domain optical coherence tomography images. *IEEE Transactions on Medical Imaging*, 28(9):1436–1447.

Glittenberg, C., Krebs, I., Falkner-Radler, C., Zeiler, F., Haas, P., Hagen, S., and Binder, S. (2009). Advantages of using a ray-traced, three-dimensional rendering system for spectral domain cirrus HD-OCT to vi-

sualize subtle structures of the vitreoretinal interface. *Ophthalmic Surgery Lasers and Imaging*, 40(2):127–134.

Götze, A., von Keyserlingk, S., Peschel, S., Jacoby, U., Schreiver, C., Köhler, B., Allgeier, S., Winter, K., Röhlig, M., Jünemann, A., Guthoff, R., Stachs, O., and Fischer, D.-C. (2018). The corneal subbasal nerve plexus and thickness of the retinal layers in pediatric type 1 diabetes and matched controls. *Scientific Reports*, 8(1).

Harrower, M. and Brewer, C. A. (2003). Colorbrewer.org: An online tool for selecting colour schemes for maps. *The Cartographic Journal*, 40(1):27–37.

Mayer, M. A., Hornegger, J., Mardin, C. Y., and Tornow, R. P. (2010). Retinal nerve fiber layer segmentation on FD-OCT scans of normal subjects and glaucoma patients. *Biomedical Optics Express*, 1(5):13581383.

Mazzaferri, J., Beaton, L., Hounye, G., N. Sayah, D., and Costantino, S. (2017). Open-source algorithm for automatic choroid segmentation of OCT volume reconstructions. *Scientific Reports*, 7.

Röhlig, M., Schmidt, C., Prakasam, R. K., Schumann, H., and Stachs, O. (2018). Visual analysis of retinal changes with optical coherence tomography. *The Visual Computer*, 34(9):1209–1224.

Schindelin, J., Rueden, C. T., Hiner, M. C., and Eliceiri, K. W. (2015). The ImageJ ecosystem: An open platform for biomedical image analysis. *Molecular Reproduction and Development*, 82(7-8):518–529.

Yoshimura, N. and Hangai, M. (2014). *OCT Atlas*. Springer, Berlin, Germany.